Check for updates

ASME Open Journal of Engineering
Online journal at:
https://asmedigitalcollection.asme.org/openengineering

Prediction of Laminar Burning Speed of Propane/Hydrogen/Air Mixtures Using Power-Law Correlation and Two Machine Learning Models

Zhenyu Lu[1]
Department of Mechanical and Industrial Engineering,
Northeastern University,
Boston, MA 02115
e-mail: lu.zhenyu@northeastern.edu

Hameed Metghalchi
Department of Mechanical and Industrial Engineering,
Northeastern University,
Boston, MA 02115
e-mail: metghalchi@coe.neu.edu

Propane (C_3H_8) and hydrogen (H_2) are regarded as alternative fuels that are favorable to the environment. Hydrogen gas's low energy density, storage, and transportation are the main issues with using it as an alternative fuel. Addition of hydrogen gas in the combustion of propane will also improve flame stability, broaden lean flammability limits, and reduces pollutant emissions. Thus, utilizing propane and hydrogen mixtures as fuel is a good choice. Laminar burning speed is a fundamental property of a combustible mixture and can be used to provide information regarding the mixture's reactivity, exothermicity, and diffusivity. In this study, power-law correlation and machine learning methods were used to create models that predict the laminar burning speed of propane/hydrogen/air mixtures at various states. Two machine learning models are artificial neural network (ANN) and support vector machine (SVM). The data were generated by using CANTRA code and a chemical kinetic mechanism. For a wide variety of input values, the models were able to determine the laminar burning speed with great accuracy. The ANN model yields the best performance. The main advantage of these models is the noticeably faster computing time when compared to chemical reaction mechanisms. [DOI: 10.1115/1.4062745]

Keywords: alternative energy sources, artificial intelligence, combustion, hydrogen energy

1 Introduction

Propane is a colorless, odorless gas that belongs to the family of hydrocarbon fuels. It is commonly used as a source of energy for various applications. Propane is derived from natural gas processing and petroleum refining. It is highly portable, easy to store, and has a high energy density, making it a popular choice for residential, commercial, and industrial purposes. Hydrogen is a colorless, odorless, and highly flammable gas at room temperature. In a variety of applications and industries, hydrogen is essential. The creation of methanol for chemicals, ammonia for fertilizers, and several other significant industrial operations all use hydrogen as a key feedstock. Additionally, hydrogen is used as a reducing agent in metallurgical processes and the refinement of fossil fuels.

Solar energy can be used to produce green hydrogen through a process called solar water splitting or photovoltaic electrolysis. This process involves using solar panels or photovoltaic cells to convert sunlight directly into electricity, which is then used to split water molecules into hydrogen (H_2) and oxygen (O_2) through electrolysis [1].

Both hydrogen and propane are regarded as alternative fuels that are favorable to the environment. Hydrogen gas's low energy density, storage, and transportation are the main issues with using it as an alternative fuel. Additionally, the addition of hydrogen to the hydrocarbon combustion process enhances flame stability, expands lean flammability limits, and lowers pollutant emissions [2]. Thus, utilizing propane and hydrogen mixtures as fuel is a good option.

Laminar burning speed is a fundamental property of a combustible mixture and can be used to provide information regarding the mixture's reactivity, exothermicity, and diffusivity. Laminar burning speed is directly dependent on fuel type, equivalence ratio, pressure, and temperature. Laminar burning speed is an important parameter in combustion research and engineering applications. It is used to characterize fuel performance, evaluate combustion efficiency, and model flame behavior in various systems. It plays a crucial role in the design and optimization of internal combustion engines, gas turbines, and other combustion devices.

There are several experimental methods to measure laminar burning speed of propane/hydrogen/air mixtures. The methods can be divided into stationary flame method and propagating flame method based on the flame type. For the stationary flame method, some commonly used burners include the Bunsen burner, the counter flow burner, and the flat flame burner. The propagating flame method also can be separated into the constant

[1]Corresponding author.

Manuscript received June 4, 2023; final manuscript received June 7, 2023; published online July 18, 2023. Special Editor: Hamid Hamidzedeh.

Copyright © 2023 by ASME; reuse license CC-BY 4.0

Downloaded from http://heattransfer.asmedigitalcollection.asme.org/openengineering/article-pdf/doi/10.1115/1.4062745/7025455/aoje_2_021038.pdf by guest on 19 July 2024

pressure method and the constant volume method [3–7]. Dirrenberger et al. [8] utilized a newly built flat flame adiabatic burner to perform laminar burning speed measurements. Tang et al. [9] measured laminar burning speeds of the propane/hydrogen/air mixtures by using the constant pressure method. Wang et al. and Yelishala et al. [10,11] used the constant volume method to measure the burning speed of propane–air–carbon dioxide at elevated temperatures and pressures. Also, the theoretical laminar burning speed can be calculated using chemical kinetic mechanisms [12,13].

Artificial intelligence (AI) refers to the simulation of human intelligence in machines that are programmed to think, learn, and perform tasks that typically require human intelligence. It encompasses a wide range of technologies and techniques that enable machines to perceive, reason, and act intelligently. Machine learning is a branch of artificial intelligence that focuses on developing algorithms and models capable of learning from data and making predictions or decisions without explicit programming. It involves the use of statistical techniques and computational algorithms to enable computers to learn and improve from experience automatically. Deep learning is a subset of machine learning that focuses on artificial neural networks inspired by the structure and function of the human brain. It leverages these neural networks, often referred to as deep neural networks, to learn and make predictions from large amounts of data.

In the last few years, artificial intelligence was introduced to combustion research. Also, it has been used in determining laminar burning speed of fuel/air mixtures. Eckart et al. [14] applied and compared some machine learning methods for the calculation of laminar burning speed for hydrogen–methane mixtures. Malik et al. [15] created a laminar burning speed model based on a deep neural network for hydrogen and propane with air. Shahpouri et al. [16] designed a model of machine learning to predict laminar burning speed of low-carbon fuels. Varghese and Kumar [17] developed a Machine learning model to predict laminar burning velocities of H_2/CO/CH_4/CO_2/N_2/air mixtures at high pressure and temperature conditions.

The goal of this paper is to predict laminar burning speeds of C_3H_8/H_2/air mixtures for a wide range of C_3H_8/H_2/air combustion conditions using power-law correlation and two machine learning models. The models were created by fitting known laminar burning speed data. The data were generated by using CANTRA code and a chemical kinetic mechanism. Results of predicted laminar burning speeds using a power-law correlation, artificial neural network (ANN), and support vector machine (SVM) have been compared in this work.

2 Data Generation

The data on laminar burning speed have been generated computationally solving one-dimensional steady-state premix flame using the CANTRA code. The chemical kinetic mechanism of USC-Mech II which has 111 species and 784 reactions relevant to C_1–C_4 hydrocarbons and syngas oxidation at high temperatures [18] was used. The data set is divided into a train set and a test set. The train set includes laminar burning speeds under different conditions (mole fractions of hydrogen, equivalence ratios, pressures, temperatures). The test set is laminar burning speeds along the isentrope. The relationship between temperature and pressure due to the isentropic process is

$$p = p_i\left(\frac{T}{T_i}\right)^{\frac{\gamma}{\gamma-1}} \tag{1}$$

where $p_i = 1$ atm is the initial pressure, $T_i = 400$ K is the initial temperature, and γ is the specific heat ratio. Hydrogen mole fraction in the fuel is defined as

$$X = \frac{N_{H_2}}{N_{H_2} + N_{C_3H_8}} \times 100\%$$

Table 1 Data set range for hydrogen mole fraction, equivalence ratio, pressure, and temperature

	Train set	Test set
Hydrogen mole fraction	0, 20%, 40%, 60%, 80%, 100%	0, 20%, 40%, 60%, 80%, 100%
Equivalence ratio	0.6, 0.8, 1, 1.2, 1.4	0.6, 0.8, 1, 1.2, 1.4
Pressure	1, 2, 3, 4, 5, 6 bar	Related to temperature
Temperature	300, 350, 400, 450, 500, 550, 600 K	425, 450, 475, 500, 525, 550, 575 K

The overall reaction of C_3H_8/H_2/air is

$$\phi((1-X)C_3H_8 + XH_2) + (5 - 4.5X)(O_2 + 3.76N_2) \rightarrow \text{products}$$

where ϕ is the fuel/air equivalence ratio.

A summary of the range of the data set is given in Table 1. Thus, burning speed of 1260 states for the train set and 210 states for the test set were calculated.

3 Methodology

Several methods have been used to fit known laminar burning speeds for C_3H_8/H_2/air mixtures and predict unknown laminar burning speeds for C_3H_8/H_2/air mixtures.

3.1 Power-Law Correlation. Metghalchi and Keck [19] experimentally determined laminar burning speeds for various fuel–air mixtures over a range of temperatures and pressures. They originally proposed a simple power-law correlation

$$S_u = S_{u0}\left(\frac{T_u}{T_{u_0}}\right)^{\alpha}\left(\frac{p}{p_0}\right)^{\beta} \tag{2}$$

The correlation has been recently expanded to provide more precise fitting

$$S_u = S_{u0}(1 + a(\phi - 1) + b(\phi - 1)^2)\left(\frac{T_u}{T_{u_0}}\right)^{\alpha_0+\alpha_1\phi}\left(\frac{p}{p_0}\right)^{\beta_0+\beta_1\phi} \tag{3}$$

where S_{u0} is the laminar burning speed at reference state ($T_{u0} = 298$ K and $p_0 = 1$ atm); a, b, α_0, α_1, β_0, and β_1 are power-law correlation coefficients. The coefficients can be determined when the mean square error (MSE) is minimum. They are found using function named *optimize.minimize* in the PYTHON SciPy package, an unconstrained minimization method. In this work, laminar burning speed for propane/hydrogen/air mixtures have been fitted in different mole fractions of hydrogen.

3.2 Artificial Neural Network. ANN is a computational model inspired by the structure and function of biological neural networks, such as the human brain. ANN is a fundamental concept within the field of artificial intelligence and machine learning.

Hyperparameters in an ANN model are parameters that are set before the training process begins and determine the behavior and performance of the network. The number of hidden layers in the network is a crucial hyperparameter. It determines the depth and complexity of the model. The number of neurons in each hidden layer is another hyperparameter. It controls the representational capacity and learning ability of the network. A loss function, also known as a cost function, is a measure that quantifies how well a machine learning model is performing on a given task. It calculates the error or discrepancy between the predicted output of the model and the true output or target value. An activation function is a mathematical function that is applied to the output of a neuron in an ANN. It introduces non-linearity to the network, allowing it to

Downloaded from http://heattransfer.asmedigitalcollection.asme.org/openengineering/article-pdf/doi/10.1115/1.4062745/7025455/aoje_2_021038.pdf by guest on 19 July 2024

learn and model complex relationships in the data. The learning rate is a hyperparameter that determines the step size at each iteration when updating the parameters of a machine learning or deep learning model during the training process. Adaptive learning-rate algorithms are optimization techniques used in machine learning and deep learning to automatically adjust the learning rate during the training process.

An ANN model is typically constructed in several steps. Here is a general description of what happens:

(1) *Data Preparation*: Compile and preprocess the data first.
(2) *Model Structure Design*: Decide the structure of the ANN. Choosing the number of layers, the number of neurons in each layer, and the activation functions to be applied are all part of this process. The type of data and the nature of the challenge will determine the structure.
(3) *Initialization*: Initialize the weights and biases of the neural network. This step randomly assigns initial values to the parameters, which will be updated during the training process to optimize the model's performance.
(4) *Forward Propagation*: Perform forward propagation to compute the output of the neural network. In this step, the input data are fed into the network, and the activation function of each active node receives the total of the input values multiplied by certain weights, as depicted in Fig. 1. Each next layer $n+1$ is connected to layer n by

$$V_i^{n+1} = f\left(\sum_{i=1}^{N} w_i^n V_i^n + b_i^n\right) \tag{4}$$

where V is the vector in each layer, w is the matrix containing the weights, vector b contains the biases, N is the number of neurons in the layer, and f is the activation function.
(5) *Loss Calculation*: Calculate the loss or error between the predicted output and the actual output. The choice of the loss (cost) function depends on the specific problem, such as MSE for regression tasks or categorical cross-entropy for classification tasks.
(6) *Backpropagation*: Perform backpropagation to propagate the error backward through the network. This step involves calculating the gradients of the loss function with respect to the weights and biases of the neural network. The gradients indicate the direction and magnitude of the updates required to minimize the loss.
(7) *Parameter Updates*: Update the weights and biases of the neural network using an optimization algorithm. The most used optimization algorithm is stochastic gradient descent (SGD), but there are also variants like Adam, RMSprop, and others. These algorithms use the calculated gradients to determine the updates that should be made to the parameters to minimize the loss.

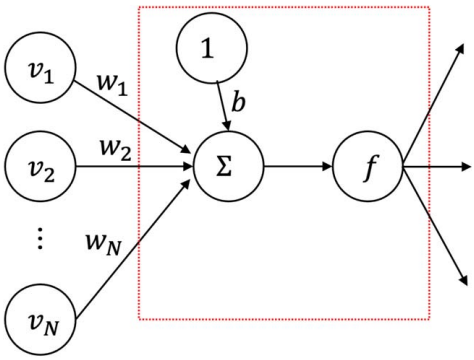

Fig. 1 Schematic diagram of a single neuron with the associated weights and bias

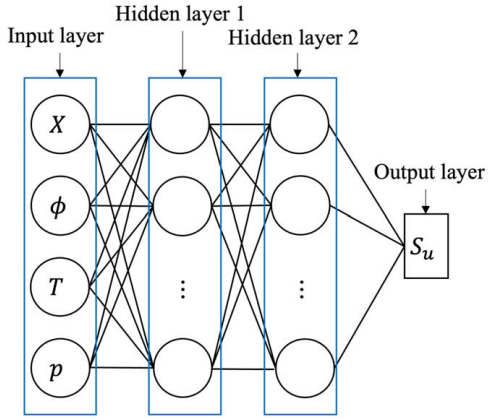

Fig. 2 Structure of ANN used in this study

(8) *Iterative Training*: Repeat Steps 4–7 iteratively for a defined number of epochs or until a convergence criterion is met. The forward propagation, loss calculation, backpropagation, and parameter updates are all carried out at each iteration to update the model's parameters and boost performance.
(9) *Model Evaluation*: Evaluate the trained model using a separate test data set or through cross-validation. Calculate performance metrics such as accuracy, precision, recall, or mean squared error, depending on the type of problem. This step enables evaluation of the model's ability to generalize to unseen data.

A Jupyter script with Pytorch is used to perform these calculations. The ANN model is used for prediction of laminar burning speed. Figure 2 shows the structure of this ANN model. It has four inputs, hydrogen mole fraction, equivalence ratio, pressure, and unburned gas temperature, two hidden layers, and one output laminar burning speed. The hyperparameters selected in this model are listed in Table 2.

3.3 Support Vector Machines. SVM is a popular supervised machine learning algorithm used for classification and regression tasks. SVMs are widely used for their effectiveness in handling both linear and non-linear data separation. The main idea behind SVM is to find an optimal hyperplane that separates data points of different classes in a high-dimensional feature space. A hyperplane is a decision boundary that maximizes the margin, or the distance, between the closest data points of different classes. The data points that are closest to the hyperplane are called support vectors. Figure 3 shows all components of SVM model. When SVM is used for regression, then it is generally referred to as support vector regression (SVR).

These computations are carried out using a Jupyter script with sklearn. The SVM model for laminar burning speed prediction also has four inputs: hydrogen mole fraction, equivalence ratio,

Table 2 Hyperparameters in the ANN model

Hyperparameter	Value
Loss (cost) function	Mean squared error (MSE) $\frac{1}{n}\sum_{i=1}^{n}(S_u - S_{u_{pred}})_i^2$
Learning rate	10^{-2}
Adaptive learning-rate algorithms	Adam
Activation function	tanh
Number of hidden layers	2
Number of neurons per hidden layer	32 for layer 1 64 for layer 2

Downloaded from http://heattransfer.asmedigitalcollection.asme.org/openengineering/article-pdf/doi/10.1115/1.4062745/7025455/aoje_2_021038.pdf by guest on 19 July 2024

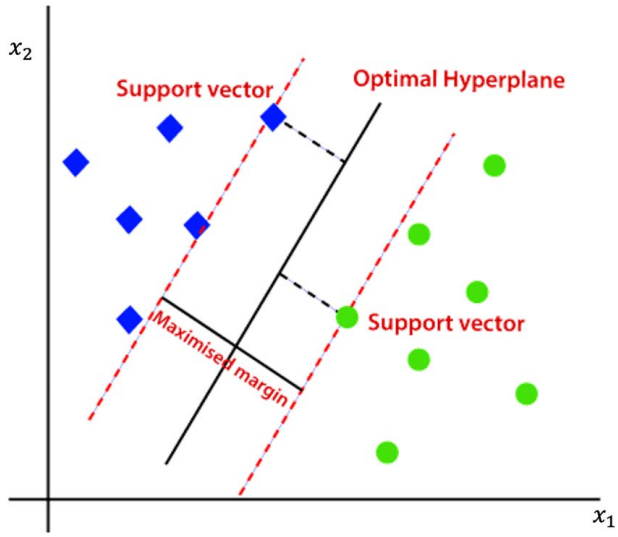

Fig. 3 All components of SVM [20]

Table 3 Hyperparameters in the SVM model

Hyperparameter	Value
Kernel function	Gaussian
Kernel coefficient (γ)	0.1
Regularization parameter (C)	1000

pressure, and unburned gas temperature. The hyperparameters selected in this model are listed in Table 3. The kernel function is to take data as input and transform it into the required form. The kernel coefficient (γ parameter) defines how far the influence of a single training example reaches, with low values meaning "far" and high values meaning "close." The regularization parameter (C parameter) trades off correct classification of training examples against maximization of the decision function's margin [21].

4 Results and Discussion

4.1 Power-Law Correlation. For the power-law correlation, laminar burning speed of propane/hydrogen/air mixtures has been fitted in different mole fractions of hydrogen. The extended equation mentioned earlier have been utilized. Equation (3) has been used to fit all data. Different set of fitting variables a, b, α_0, α_1, β_0, and, β_1 have been determined for different mole fraction of hydrogen. The coefficients for different hydrogen each fraction are shown in Table 4.

Table 5 shows the MSE and coefficient of determination (R^2) of the train set and test set as well as the average relative error of power-law correlation for different hydrogen mole fraction.

The relative error is somehow high for all the cases of this methods. Because of that the machine learning methods have been used to fit the data and predict the laminar burning speed.

The developed machine learning models for laminar burning speed prediction have four inputs: hydrogen mole fraction, equivalence ratio, pressure, and unburned gas temperature, and the output is predicted laminar burning speed.

4.2 Artificial Neural Network. For the ANN model, the MSE and coefficient of determination (R^2) of the train set and test set as well as the average relative error are listed in Table 6. It can be seen that the coefficient of determination (R^2) is very close to 1 which means that the ANN model perfectly predicts the outcome. Table 6 also shows the error is less than 1%, making it almost a perfect fit.

4.3 Support Vector Machines. For the SVM model, two data sets were used. One of the data sets does not contain the data under the condition that the hydrogen mole fraction is 100%. The other data set contains the data under this condition which is the whole data set mentioned previously. The MSE, coefficient of determination (R^2), and the average relative error of the two data sets are listed in Table 7. For the whole data set, the MSE and relative error are quite significant, making it not a good fit; but, for a part of the data set, it is a decent fitting. The partial data set's coefficient of determination (R^2) is quite near 1, indicating that the SVM model accurately predicts the result. The following result is based on the partial data set.

4.4 Comparison of Methods. The primary benefit of these methods is the significantly faster computation time when compared to solving one-dimensional premixed flame with a chemical reaction mechanism. As an example, the run time using the chemical reaction mechanism to predict the laminar burning speed of C_3H_8/H_2/air mixtures is around 30 s, and the run time using the ANN model and SVM model to predict the laminar burning speed of C_3H_8/H_2/air mixtures is around 2–3 milliseconds. The computations were done with Apple M1 chip with eight-core CPU, 8-core GPU, and 16-core Neural Engine. Based on the Tables 6 and 7, both the ANN model and SVM model show good predictive accuracy over a wide range of conditions. The ANN model has a better prediction performance than the SVM model.

Figure 4 shows the laminar burning speed of propane air mixture with zero hydrogen at 1 atm pressure and temperature of 298 K as a function of fuel/air equivalence ratio. Comparison of theoretical laminar burning speeds of C_3H_8/H_2/air with predicted laminar burning speeds of three methods is performed. Also, included, are measured values of burning speed by a few researchers. It can be seen that the ANN method has the best prediction followed by the SVM method.

Figure 5 shows the burning speed of propane/hydrogen/air mixtures at 1 atm pressure, temperature of 298 K, and hydrogen mole fraction of 20% as a function of fuel/air equivalence ratio. It can be seen that the equivalence ratio at which the burning speed is maximum slightly shift to richer mixture. The two AI models almost predict the same values for burning speeds while power law fit under-predicts the burning speed as it does for hydrogen mole fraction of zero.

Figures 6–8 predict the burning speeds of propane/hydrogen/ air mixtures at a temperature of 298 K, a pressure of 1 atm, and

Table 4 Power-law correlation coefficients

	S_{u_0}	a	b	α_0	α_1	β_0	β_1
0	0.3424	0.1007	−2.9337	1.8010	0.1661	−0.2764	−0.0188
20%	0.3601	0.1233	−2.8758	1.7938	0.1707	−0.2747	−0.0209
40%	0.3886	0.1622	−2.7874	1.7855	0.1767	−0.2748	−0.0210
60%	0.4432	0.2405	−2.6181	1.7963	0.1613	−0.2763	−0.0179
80%	0.5905	0.4486	−2.2068	1.8952	0.0542	−0.2821	−0.0050
100%	1.9973	1.1980	−0.6930	2.7784	−0.8282	−0.3638	0.2530

Downloaded from http://heattransfer.asmedigitalcollection.asme.org/openengineering/article-pdf/doi/10.1115/1.4062745/7025455/aoje_2_021038.pdf by guest on 19 July 2024

Table 5 Mean square error (MSE) and coefficient of determination (R^2) as well as average relative error for power-law correlation

	MSE		R^2		
	Train set	Test set	Train set	Test set	Relative error
0	6.0048E-04	1.2902E-04	0.9907	0.9949	6.91%
20	6.7539E-04	1.5438E-04	0.9905	0.9944	6.91%
40	7.9722E-04	2.0259E-04	0.9904	0.9935	6.88%
60	1.0560E-03	3.0261E-04	0.9903	0.9923	6.71%
80	1.8157E-03	6.8564E-04	0.9912	0.9911	6.04%
100	2.5024E-02	6.3119E-03	0.9942	0.9977	5.05%

Table 6 The Mean square error (MSE) and coefficient of determination (R^2) of the ANN model

	MSE		R^2		
	Train set	Test set	Train set	Test set	Relative error
ANN	6.653E-05	1.044E-04	0.99997	0.99994	0.92%

Table 7 The Mean square error (MSE) and coefficient of determination (R^2) of the SVM model

	MSE		R^2		
	Train set	Test set	Train set	Test set	Relative error
Partial set	2.710E-04	2.486E-04	0.9978	0.9965	1.96%
Whole set	0.2513	0.2626	0.9101	0.9045	35.3%

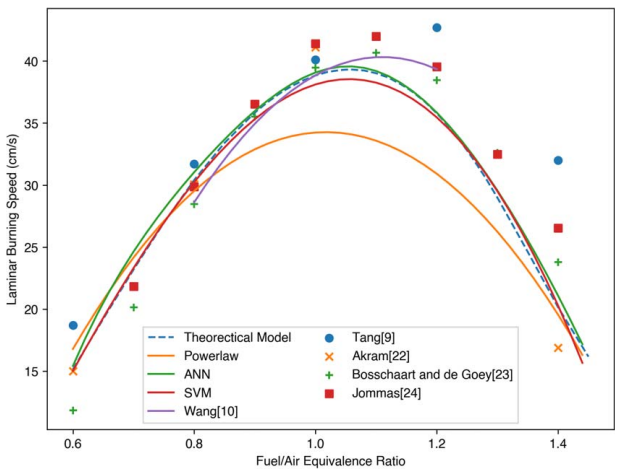

Fig. 4 Comparison of theoretical laminar burning speeds of C_3H_8/H_2/air mixtures versus predicted laminar burning speeds of three methods and previous experimental results [10,9,22–24]. The pressure is 1 atm, the temperature is 298 K, and the mole fraction of hydrogen is 0.

hydrogen mole fractions of 40%, 60%, and 80%. It can be seen that the two AI methods are great, the fuel/air equivalence ratio where burning speed is maximum to richer mixtures. This is because hydrogen burning speed is maximum at a very rich mixture. Also, values of burning speeds increase as percentages of hydrogen increase in the fuel mixture. This is due to having a very high burning speed for hydrogen.

Figures 9–13 show a comparison of theoretical laminar burning speeds of C_3H_8/H_2/air with predicted laminar burning speeds of three methods. In these figures, burning speeds are shown as a

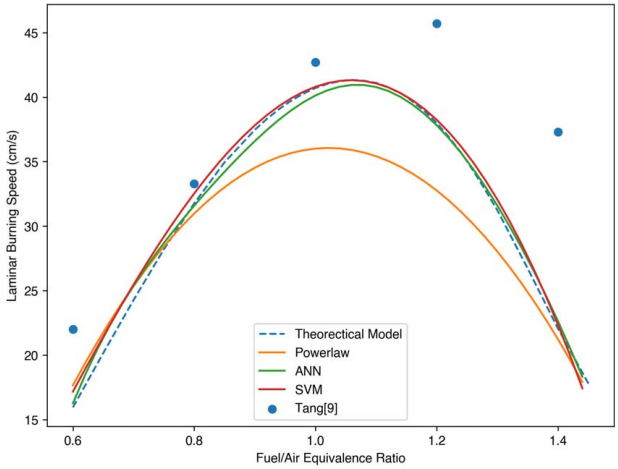

Fig. 5 Comparison of theoretical laminar burning speeds of C_3H_8/H2/air mixtures versus predicted laminar burning speeds of three methods and previous experimental results [9]. The pressure is 1 atm, the temperature is 298 K, and the mole fraction is 20%.

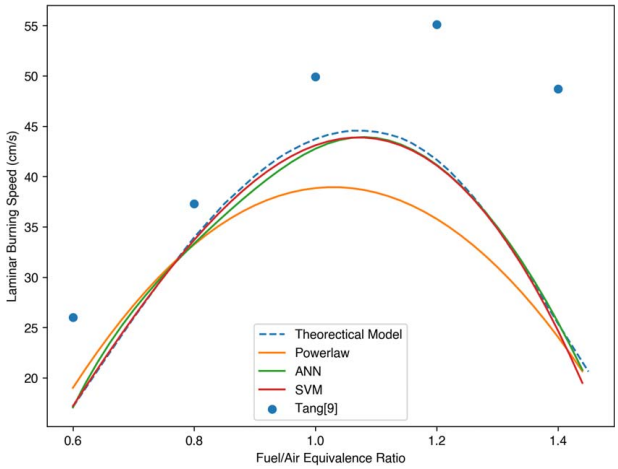

Fig. 6 Comparison of theoretical laminar burning speeds of C_3H_8/H_2/air mixtures versus predicted laminar burning speeds of three methods and previous experimental results [9]. The pressure is 1 atm, the temperature is 298 K, and the mole fraction of hydrogen is 40%.

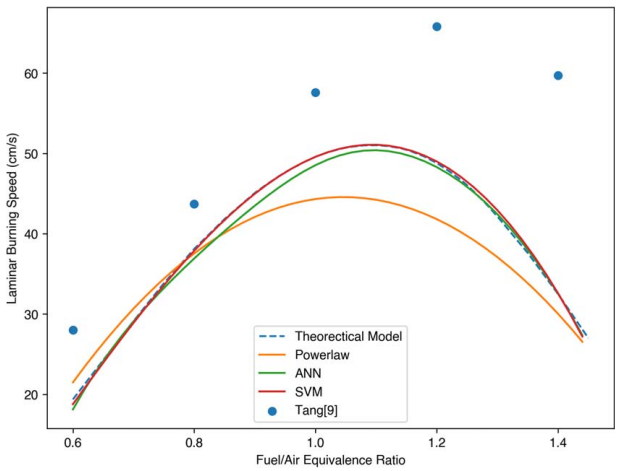

Fig. 7 Comparison of theoretical laminar burning speeds of C_3H_8/H_2/air mixtures versus predicted laminar burning speeds of three methods and previous experimental results [9]. The pressure is 1 atm, the temperature is 298 K, and the mole fraction of hydrogen is 60%.

Downloaded from http://heattransfer.asmedigitalcollection.asme.org/openengineering/article-pdf/doi/10.1115/1.4062745/7025455/aoje_2_021038.pdf by guest on 19 July 2024

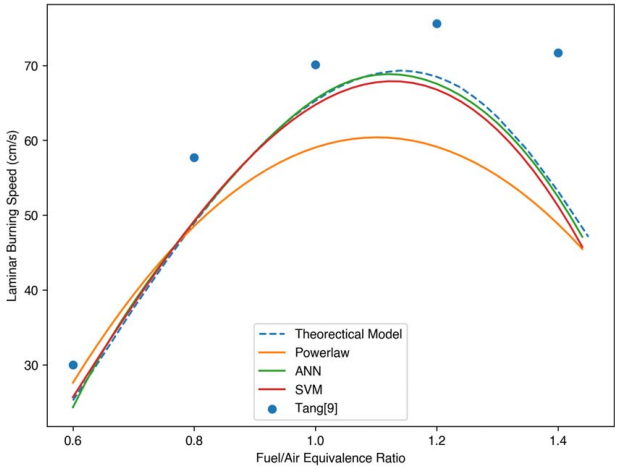

Fig. 8 Comparison of theoretical laminar burning speeds of C_3H_8/H_2/air mixtures versus predicted laminar burning speeds of three methods and previous experimental results [9]. The pressure is 1 atm, the temperature is 298 K, and the mole fraction of hydrogen is 80%.

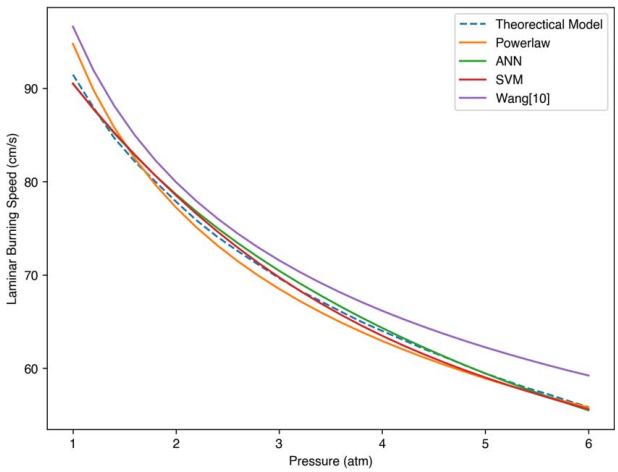

Fig. 9 Comparison of theoretical laminar burning speeds of C_3H_8/H_2/air mixtures versus predicted laminar burning speeds of three methods and previous experimental results [10] versus pressure. The equivalence ratio is 1, the temperature is 500 K, and the mole fraction of hydrogen is 0.

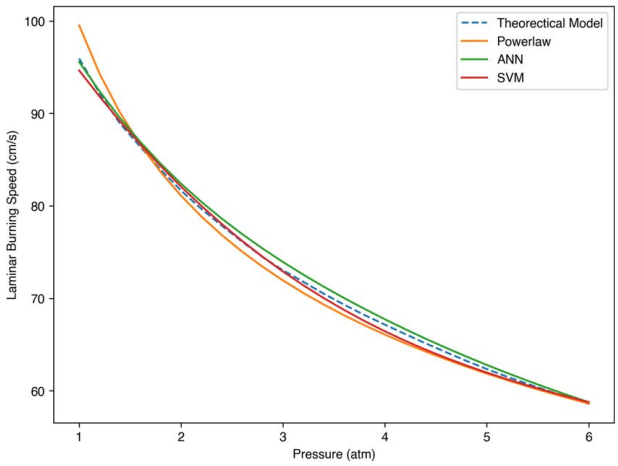

Fig. 10 Comparison of theoretical laminar burning speeds of C_3H_8/H_2/air mixtures versus predicted laminar burning speeds of three methods versus pressure. The equivalence ratio is 1, the temperature is 500 K, and the mole fraction of hydrogen is 20%

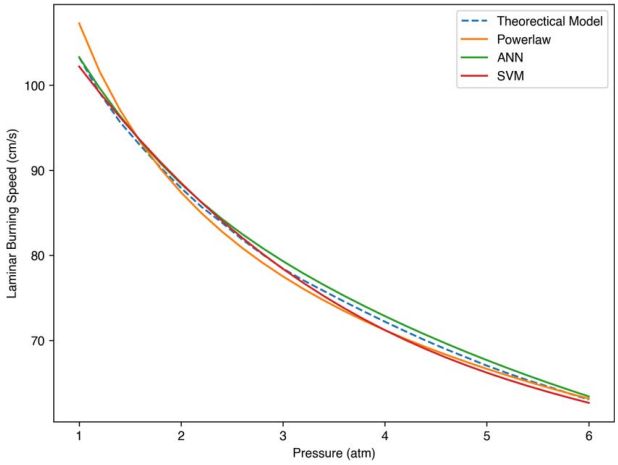

Fig. 11 Comparison of theoretical laminar burning speeds of C_3H_8/H_2/air mixtures versus predicted laminar burning speeds of three methods versus pressure. The equivalence ratio is 1, the temperature is 500 K, and the mole fraction of hydrogen is 40%.

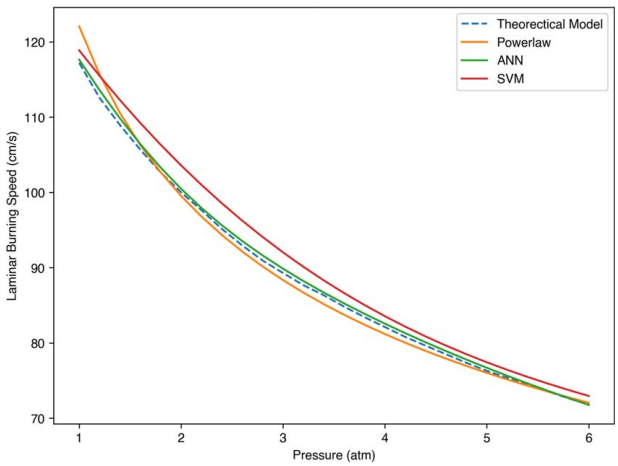

Fig. 12 Comparison of theoretical laminar burning speeds of C_3H_8/H_2/air mixtures versus predicted laminar burning speeds of three methods. Versus pressure. The equivalence ratio is 1, the temperature is 500 K, and the mole fraction of hydrogen is 60%.

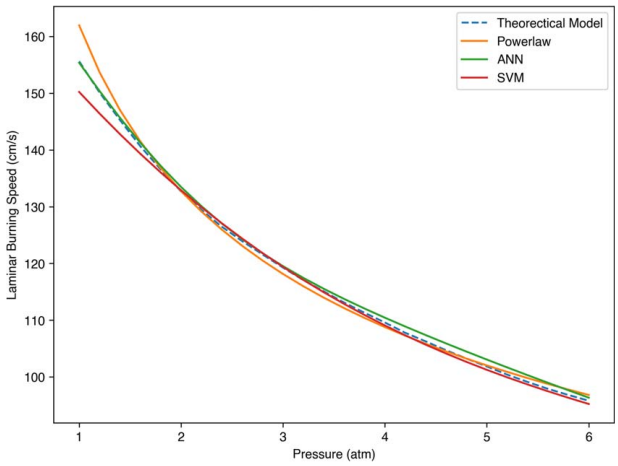

Fig. 13 Comparison of theoretical laminar burning speeds of C_3H_8/H_2/air mixtures versus predicted laminar burning speeds of three methods as a function of pressure. The equivalence ratio is 1, the temperature is 500 K, and the mole fraction of hydrogen is 80%.

Downloaded from http://heattransfer.asmedigitalcollection.asme.org/openengineering/article-pdf/doi/10.1115/1.4062745/7025455/aoje_2_021038.pdf by guest on 19 July 2024

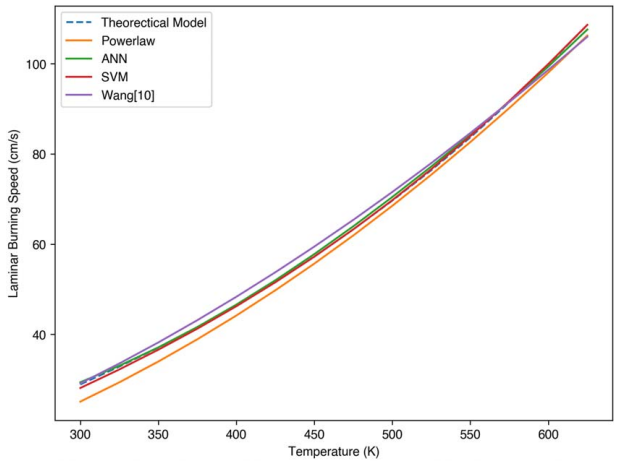

Fig. 14 Comparison of theoretical laminar burning speeds of C_3H_8/H_2/air mixtures versus predicted laminar burning speeds of three methods and previous experimental results [10]. The equivalence ratio is 1, the pressure is 3 atm, and the mole fraction of hydrogen is 0.

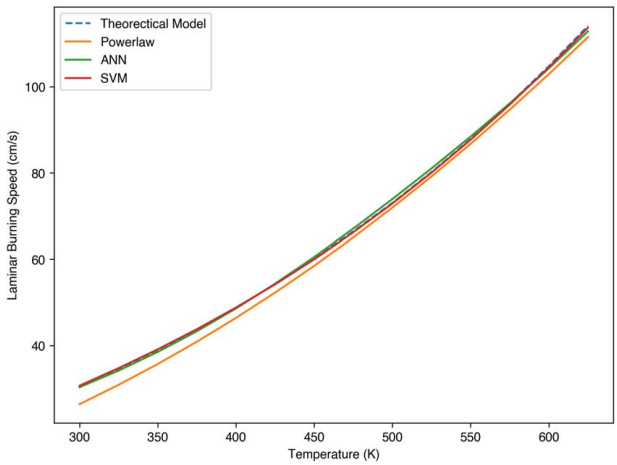

Fig. 15 Comparison of theoretical laminar burning speeds of C_3H_8/H_2/air mixtures versus predicted laminar burning speeds of three methods. The equivalence ratio is 1, the pressure is 3 atm, and the mole fraction of hydrogen is 20%.

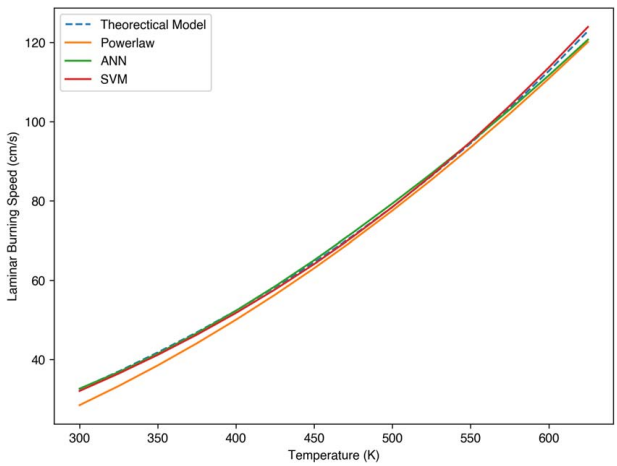

Fig. 16 Comparison of theoretical laminar burning speeds of C_3H_8/H_2/air mixtures versus predicted laminar burning speeds of three methods. The equivalence ratio is 1, the pressure is 3 atm, and the mole fraction of hydrogen is 40%.

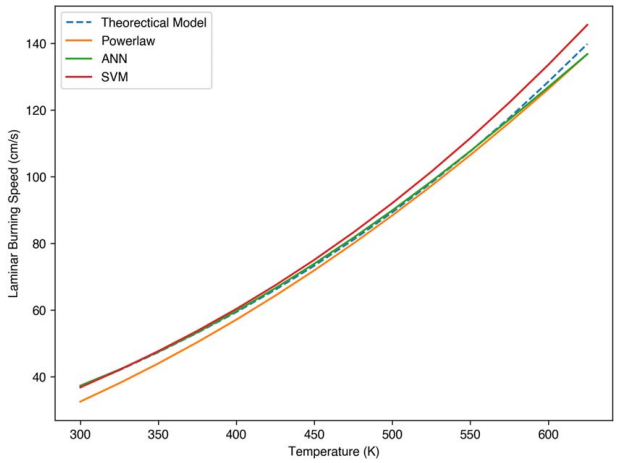

Fig. 17 Comparison of theoretical laminar burning speeds of C_3H_8/H_2/air mixtures versus predicted laminar burning speeds of three methods. The equivalence ratio is 1, the pressure is 3 atm, and the mole fraction of hydrogen is 60%.

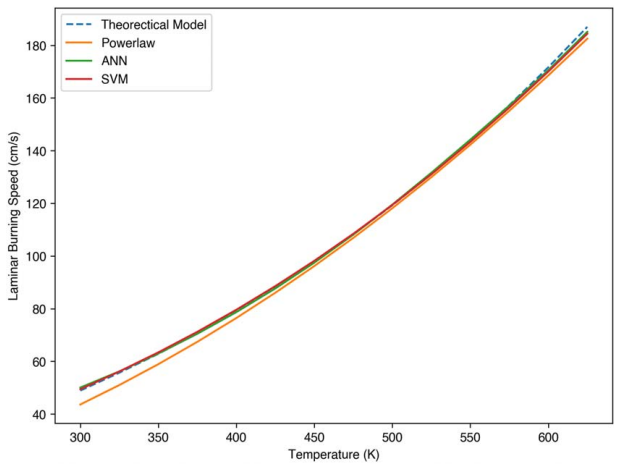

Fig. 18 Comparison of theoretical laminar burning speeds of C_3H_8/H_2/air mixtures versus predicted laminar burning speeds of three methods. The equivalence ratio is 1, the pressure is 3 atm, and the mole fraction of hydrogen is 80%.

function of pressure for stoichiometric mixtures and temperature of 500 K. Mole fraction of hydrogen is zero in Fig. 9, 20% in Fig. 10, 40% in Fig. 11, 60% in Fig. 12, and 80% in Fig. 13. Figure 9 also shows the experimental results of Wang [9]. It can be seen that at a high temperature of 500 K, the power-law correlation (Eq. (3)) and both AI models predict burning speed values relatively fine. It also can be seen that as pressure increases, burning speed decreases and Eq. (3) shows this clearly as the pressure exponent is negative. It can also be seen that burning speed increases as the mole fraction of hydrogen increases.

Figures 14–18 show that the theoretical values have been compared with three predicted results of correlation (Eq. (3)) and two AI models. Also, the experimental results of Wang et al. [10] are included in Fig. 14. These comparisons have been made for stoichiometric mixtures having a pressure of 3 atmosphere with a wide range of temperatures. All three fits are fine with the ANN method slightly better. It can be observed that burning speed is a very strong function of temperature as is evident by having a positive number of about 2 for temperature exponents in the correlation (Eq. (3)). This is true for all hydrogen mixtures. Also, these figures show the burning speeds of the mixtures increase as the percentage of hydrogen in the mixture is increased.

Downloaded from http://heattransfer.asmedigitalcollection.asme.org/openengineering/article-pdf/doi/10.1115/1.4062745/7025455/aoje_2_021038.pdf by guest on 19 July 2024

5 Conclusion

In this work, several methods including power-law correlation and machine learning techniques have been used to fit known laminar burning speeds for C_3H_8/H2/air mixtures and achieve a function or model to predict unknown laminar burning speeds of fuel/air mixtures. The input of this function or model is the hydrogen mole fraction, equivalence ratio, pressure, and unburned gas temperature. For a wide variety of input values, the models were able to determine the laminar burning speed with great accuracy. The ANN model yields the best performance. The main advantage of these models is the noticeably faster computing time when compared to chemical reaction mechanisms.

Conflict of Interest

There are no conflicts of interest. This article does not include research in which human participants were involved. Informed consent is not applicable. This article does not include any research in which animal participants were involved.

Data Availability Statement

The data sets generated and supporting the findings of this article are obtainable from the corresponding author upon reasonable request.

References

[1] Udousoro, D. A., and Dansoh, C., 2020, "Production of Hydrogen Using Solar-Powered Electrolysis," Renewable Energy and Sustainable Buildings: Selected Papers From the World Renewable Energy Congress *WREC 2018*, A. Sayigh, ed., Springer International Publishing, Cham, pp. 431–447.

[2] Hawkes, E. R., and Chen, J. H., 2004, "Direct Numerical Simulation of Hydrogen-Enriched Lean Premixed Methane–Air Flames," Combust. Flame, **138**(3), pp. 242–258.

[3] Bai, Z., Wang, Z., Yu, G., Yang, Y., and Metghalchi, H., 2019, "Experimental Study of Laminar Burning Speed for Premixed Biomass/Air Flame," ASME J. Energy Resour. Technol., **141**(2), p. 022206.

[4] Moghaddas, A., Bennett, C., Eisazadeh-Far, K., and Metghalchi, H., 2012, "Measurement of Laminar Burning Speeds and Determination of Onset of Auto-Ignition of Jet-A/Air and Jet Propellant-8/Air Mixtures in a Constant Volume Spherical Chamber," ASME J. Energy Resour. Technol., **134**(2), p. 022205.

[5] Wang, Z., Alswat, M., Yu, G., Allehaibi, M. O., and Metghalchi, H., 2017, "Flame Structure and Laminar Burning Speed of Gas to Liquid Fuel Air Mixtures at Moderate Pressures and High Temperatures," Fuel, **209**, pp. 529–537.

[6] Wang, Z., Lu, Z., Yelishala, S. C., Metghalchi, H., and Levendis, Y. A., 2020, "Laminar Burning Speeds and Flame Instabilities of Isobutane Carbon Dioxide Air Mixtures at High Pressures and Temperatures," Fuel, **268**, p. 117410.

[7] Eisazadeh-Far, K., Parsinejad, F., and Metghalchi, H., 2010, "Flame Structure and Laminar Burning Speeds of JP-8/Air Premixed Mixtures at High Temperatures and Pressures," Fuel, **89**(5), pp. 1041–1049.

[8] Dirrenberger, P., Le Gall, H., Bounaceur, R., Herbinet, O., Glaude, P.-A., Konnov, A., and Battin-Leclerc, F., 2011, "Measurements of Laminar Flame Velocity for Components of Natural Gas," Energy Fuels, **25**(9), pp. 3875–3884.

[9] Tang, C., Huang, Z., Jin, C., He, J., Wang, J., Wang, X., and Miao, H., 2008, "Laminar Burning Velocities and Combustion Characteristics of Propane–Hydrogen–Air Premixed Flames," Int. J. Hydrogen Energy, **33**(18), pp. 4906–4914.

[10] Wang, Z., Lu, Z., Yelishala, S. C., Metghalchi, H., and Levendis, Y. A., 2021, "Flame Characteristics of Propane-Air-Carbon Dioxide Blends at Elevated Temperatures and Pressures," Energy, **228**, p. 120624.

[11] Yelishala, S. C., Wang, Z., Metghalchi, H., Levendis, Y. A., Kannaiyan, K., and Sadr, R., 2019, "Effect of Carbon Dioxide on the Laminar Burning Speed of Propane–Air Mixtures," ASME J. Energy Resour. Technol., **141**(8), p. 082205.

[12] Lu, Z., and Metghalchi, H., 2023, "Theoretical Prediction of Laminar Burning Speed of Normal-Decane and Jet Propellant 8," ASME J. Energy Resour. Technol., **145**(1), p. 012301.

[13] Yu, G., Askari, O., and Metghalchi, H., 2018, "Theoretical Prediction of the Effect of Blending JP-8 With Syngas on the Ignition Delay Time and Laminar Burning Speed," ASME J. Energy Resour. Technol., **140**(1), p. 012204.

[14] Eckart, S., Prieler, R., Hochenauer, C., and Krause, H., 2022, "Application and Comparison of Multiple Machine Learning Techniques for the Calculation of Laminar Burning Velocity for Hydrogen-Methane Mixtures," Ther. Sci. Eng. Prog., **32**, p. 101306.

[15] Malik, K., Żbikowski, M., and Teodorczyk, A., 2020, "Laminar Burning Velocity Model Based on Deep Neural Network for Hydrogen and Propane With Air," Energies, **13**(13), p. 3381.

[16] Shahpouri, S., Norouzi, A., Hayduk, C., Fandakov, A., Rezaei, R., Koch, C. R., and Shahbakhti, M., 2023, "Laminar Flame Speed Modeling for Low Carbon Fuels Using Methods of Machine Learning," Fuel, **333**, p. 126187.

[17] Varghese, R. J., and Kumar, S., 2020, "Machine Learning Model to Predict the Laminar Burning Velocities of H_2/CO/CH_4/CO_2/N_2/Air Mixtures at High Pressure and Temperature Conditions," Int. J. Hydrogen Energy, **45**(4), pp. 3216–3232.

[18] Wang, H., You, X., Joshi, A. V., Davis, S. G., Laskin, A., Egolfopoulos, F., and Law, C. K., 2007, "USC Mech Version II. High-Temperature Combustion Reaction Model of H2/CO/C1-C4 Compounds," http://ignis.usc.edu/Mechanisms/USC-Mech%20II/USC_Mech%20II.htm. Accessed July 28, 2022.

[19] Metghalchi, M., and Keck, J. C., 1980, "Laminar Burning Velocity of Propane-Air Mixtures at High Temperature and Pressure," Combust. Flame, **38**, pp. 143–154.

[20] Saini, A., 2021, "Support Vector Machine (SVM): A Complete Guide for Beginners," https://www.analyticsvidhya.com/.

[21] Pedregosa, F., Varoquaux, G., Gramfort, A., Michel, V., Thirion, B., Grisel, O., Blondel, M., et al., 2011, "Scikit-Learn: Machine Learning in Python," J. Mach. Learn. Res., **12**, pp. 2825–2830.

[22] Akram, M., Kishore, V. R., and Kumar, S., 2012, "Laminar Burning Velocity of Propane/CO2/N2–Air Mixtures at Elevated Temperatures," Energy Fuels, **26**(9), pp. 5509–5518.

[23] Bosschaart, K. J., and de Goey, L. P. H., 2004, "The Laminar Burning Velocity of Flames Propagating in Mixtures of Hydrocarbons and Air Measured With the Heat Flux Method," Combust. Flame, **136**(3), pp. 261–269.

[24] Jomaas, G., Zheng, X. L., Zhu, D. L., and Law, C. K., 2005, "Experimental Determination of Counterflow Ignition Temperatures and Laminar Flame Speeds of C2–C3 Hydrocarbons at Atmospheric and Elevated Pressures," Proc. Combust. Inst., **30**(1), pp. 193–200.

Downloaded from http://heattransfer.asmedigitalcollection.asme.org/openengineering/article-pdf/doi/10.1115/1.4062745/7025455/aoje_2_021038.pdf by guest on 19 July 2024